RankIQA: Learning from Rankings for No-reference Image Quality Assessment

Xialei Liu
Computer Vision Center
Barcelona, Spain
xialei@cvc.uab.es

Joost van de Weijer
Computer Vision Center
Barcelona, Spain
joost@cvc.uab.es

Andrew D. Bagdanov
MICC, University of Florence
Florence, Italy
andrew.bagdanov@unifi.it

Abstract

We propose a no-reference image quality assessment (NR-IQA) approach that learns from rankings (RankIQA). To address the problem of limited IQA dataset size, we train a Siamese Network to rank images in terms of image quality by using synthetically generated distortions for which relative image quality is known. These ranked image sets can be automatically generated without laborious human labeling. We then use fine-tuning to transfer the knowledge represented in the trained Siamese Network to a traditional CNN that estimates absolute image quality from single images. We demonstrate how our approach can be made significantly more efficient than traditional Siamese Networks by forward propagating a batch of images through a single network and backpropagating gradients derived from all pairs of images in the batch. Experiments on the TID2013 benchmark show that we improve the state-of-the-art by over 5%. Furthermore, on the LIVE benchmark we show that our approach is superior to existing NR-IQA techniques and that we even outperform the state-of-the-art in full-reference IQA (FR-IQA) methods without having to resort to high-quality reference images to infer IQA.

1. Introduction

Images are everywhere in our life. Unfortunately, they are often distorted by the processes of acquisition, transmission, storage, and external conditions like camera motion. Image Quality Assessment (IQA) [34] is a technique developed to automatically predict the perceptual quality of images. IQA estimates should be highly correlated with quality assessments made by a range of very many human evaluators (commonly referred to as the Mean Opinion Score (MOS) [27, 22]). IQA has been widely applied to problems where image quality is essential, like image restoration [13], image super-resolution [32], and image retrieval [37]. IQA approaches are generally divided into three categories based on whether the undistorted image (called reference image) or information about it is available: full-
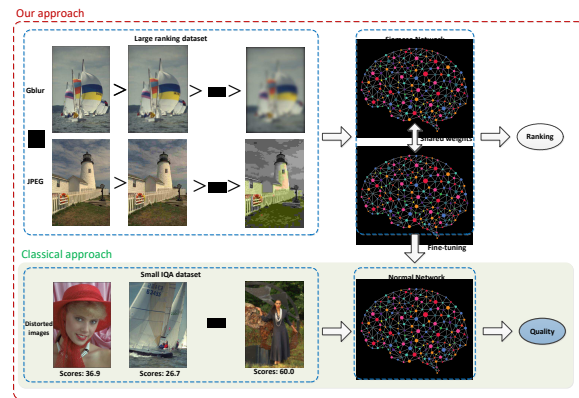

Figure 1. The classical approach trains a deep CNN regressor *directly* on the ground-truth. Our approach trains a network from an image *ranking* dataset. These ranked images can be easily generated by applying distortions of varying intensities. The network parameters are then transferred to the regression network for fine-tuning. This allows for the training of deeper and wider networks.

reference IQA (FR-IQA), reduced-reference IQA (RR-IQA), and no-reference IQA (NR-IQA). Research has mostly focussed on the more realist scenario of NR-IQA where the image quality of an image without any reference image has to be estimated. In NR-IQA, many methods focus on a specific distortion [38, 7], which limits the applicability of these methods. Other methods consider a range of distortions [20, 23, 18, 19].

Convolutional Neural Networks (CNNs) are having an enormous impact on computer vision research and practice. Though they have been around for decades [16], it wasn't until 2012, when Krizhevsky et al. [14] achieved spectacular results with a CNN in the ImageNet competition, that they achieved wide attention and adoption in the broader computer vision community. The architectures of networks are getting deeper and deeper with respect to the original AlexNet, with ResNet being an example of very deep network architecture [8]. The result of this trend is that state-of-the-art CNNs like AlexNet and ResNet have hundred of

millions of parameters and require massive amounts of data to train from scratch (without overfitting).

The success of CNNs encouraged research exploring their potential application to the NR-IQA problem. This research resulted in significant improvements compared to previous hand-crafted approaches [17, 11, 12]. The main problems these papers had to address is the absence of large datasets for IQA . Especially as networks grow deeper and wider, the number of parameters increases dramatically. As a consequence, larger and larger annotated datasets are required for training. However, the annotation process for IQA image datasets requires multiple human annotations for every image, and thus the collection process is extremely labor-intensive and costly. As a results, most available IQA datasets are too small to be effective for training CNNs.

We propose an approach to address the absence of large datasets. The main idea (see Fig. 1) is that while human-annotated IQA data is difficult to obtain, it is easy to *generate* images that are *ranked* according to their image quality. That is, we can generate image sets in which, though we do not have an absolute quality measure for each generated image, for any *pair* of images we know which is of higher quality. We call this *learning from rankings* approach RankIQA, and with it we learn to rank image in terms of quality using Siamese Networks, and then we transfer knowledge learned from ranked images to a traditional CNN fine-tuned on IQA data in order to improve the accuracy of IQA. The idea to learn IQA features from distorted reference images was proposed by Zhang et al. in a patent [44]. In this paper we go beyond this patent in that we provide a detailed description of our method and experimentally verify the usefulness of pre-training networks using ranked datasets.

As a second contribution we propose a method for efficient backpropagation in Siamese networks. The method forwards a batch of images through a single network and then backpropagates gradients derived from all pairs in the batch. In extensive experiments on established IQA datasets we show that learning from rankings significantly improves results, and that our efficient backpropagation algorithm allows to train these networks better and faster than other training protocols, like hard-negative mining.

2. Related work

We briefly review the literature related to our approach. We focus on distortion-generic NR-IQA since it is more generally applicable than the other IQA research lines.

Traditional NR-IQA approaches. Most traditional NR-IQA can be classified into Natural Scene Statistics (NSS) methods and learning-based methods. In NSS methods, the assumption is that images of different quality vary in the statistics of responses to specific filters. Wavelets [20], DCT [23] and Curvelets [18] are commonly used to extract the features in different sub-bands. These feature distributions are parametrized, for example with the Generalized Gaussian Distribution [26]. The aim of these methods is to estimate the distributional parameters, from which a quality assessment can be inferred. The authors of [19] propose to extract NSS features in the spatial domain to obtain significant speed-ups. In learning-based methods, local features are extracted and mapped to the MOS using, for example, Support Machine Regression or Neural Networks [4]. The codebook method [40, 39] combines different features instead of using local features directly. Datasets without MOS can be exploited to construct the codebook by means of unsupervised learning, which is particularly important due to of the small size of existing datasets. Saliency maps [43] can be used to model human vision system and improve precision in these methods.

Deep learning for NR-IQA. In recent years several works have used deep learning for NR-IQA [1, 11, 12]. One of the main drawbacks of deep networks is the need for large labeled datasets, which are currently not available for NR-IQA research. To address this problem Kang et al. [11] consider small 32×32 patches rather than images, thereby greatly augmenting the number of training examples. The authors of [2, 12] follow the same pipeline. In [12] the authors design a multi-task CNN to learn the type of distortions and image quality simultaneously. Bianco at al. [1] propose to use a pre-trained network to mitigate the lack of training data. They extract features from a pre-trained model fine-tuned on an IQA dataset. These features are then used to train an SVR model to map features to IQA scores.

In our paper, we propose a radically different approach to address the lack of training data: we use a large number of automatically generated rankings of image quality to train a deep network. This allows us to train much deeper and wider networks than other methods in NR-IQA which train directly on absolute IQA data.

Learning to rank. These approaches learn a ranking function from ground-truth rankings by minimizing a ranking loss [3]. This function can then be applied to rank test objects. The authors of [25] adapt the Stochastic Gradient Descent method to perform pairwise learning to rank. This has been successfully applied to large datasets. Combining ideas from ranking and CNNs, the Siamese network architecture achieves great success on the face verification problem [5], and in comparing image patches [41]. The only other work which applies rankings in the context of NR-IQA is [6] in which they combine different hand-crafted features to represent image pairs from the IQA dataset.

Our approach is different in that primarily we are not aiming to learn rankings. Instead we use learning from rankings as a data augmentation technique: we use easily obtainable datasets of ranked images to train a large net-

work, which is then fine-tuned for the task of NR-IQA.

Hard-negative mining for Siamese network training. It is well known that a naive approach to sampling pairs to training Siamese networks is suboptimal. To address this problem several approaches to hard-negative mining have been proposed. In [29], they propose a hard positive and hard-negative mining strategy to forward-propagate a set of pairs and sample the highest loss pairs with back-propagation. However, hard mining comes with a high computational cost (they report an increase of up to 80% of total computation cost). In [24] they propose semi-hard pair selection, arguing that selecting hardest pairs can lead to bad local minima. The batch size used is around 1800 examples, which again leads to a considerable increase in computational cost. In [33] the authors take a batch of pairs as input and choose the four hardest negative samples within the mini-batch. To solve for a bad local optimum, [31] optimize a smooth upper bound loss function to take advantage of all possible pairs in the mini-batch.

In contrast with these works, we propose a method for efficient Siamese backpropagation which does not depend on hard-negative selection. Instead, it considers all possible pairs in the mini-batch. This has the advantage that the main computational bottleneck in training deep networks, namely the forward-propagation of images through the network, is optimally exploited.

3. Learning from rankings for NR-IQA

In this section we describe our approach to exploiting synthetically generated rankings for NR-IQA. We first lay out a general framework for our approach, then describe how we use a Siamese network architecture to learn from rankings. Finally, in section 3.3 we show how backpropagation for training Siamese networks from ranked samples can be made significantly more efficient.

3.1. Overview of our approach

The lack of large IQA datasets motivates us to propose a new strategy to take advantage of large, *unlabelled* databases from which we can generate images ranked by image quality. Our approach is based on the observation that, given a set of arbitrary reference images, it is very easy to apply image distortions to generate a *ranking* image dataset. As an example, given a reference image we can apply various levels of Gaussian blur. The set of images which is thus generated can be easily ranked because we do know that adding Gaussian blur (or any other distortion) always deteriorates the quality score. Note that in such set of ranked images we do not have any absolute IQA scores for any images – but we do know for any pair of images *which is of higher quality*.

After learning on these ranked images, we can use fine-

tuning on small image quality datasets in order to address the IQA problem. The difference between our approach and the straightforward, classical approach [12] is shown in Fig. 1. The standard approach trains a shallow network directly on the IQA dataset to estimate IQA score from images. Due to the limited data only few layers can be used, which limits accuracy. Since we have access to much larger datasets with ranked images, we can now train deeper and wider networks to learn a distance embedding. Next we follow this by fine-tuning for domain adaptation to the absolute IQA problem. The overall pipeline of our approach is:

1. **Synthesize ranked images.** Using an arbitrary set of images, we synthetically generate deformations of these images over a range of distortion intensities. The absolute distortion amount for each image is not used in subsequent steps, but within each deformation type we know, for any pair of images, which is of higher quality. See section 4.1 for a description of the datasets used for generating ranked images and the distortions applied.

2. **Train Siamese network for ranking.** Using the set of ranked images, we train a Siamese network described in the next section using the efficient Siamese backpropagation technique proposed in section 3.3. The result is a Siamese network that *ranks* images by image quality.

3. **Fine-tune on IQA data.** Finally, we extract a single branch of the Siamese network (we are interested at this point in the representation learned in the network, and not in the ranking itself), and fine-tune it on available IQA data. This effectively calibrates the network to output IQA measurements.

3.2. Siamese networks for ranking

Here we introduce the Siamese network [5] to learn from image rankings, which is a network with two identical network branches and a loss module. The two branches share weights during training. Pairs of images and labels are the input of the network, yielding two outputs which are passed to the loss module. The gradients of the loss function with respect to all model parameters are computed by backpropagation and updated with the stochastic gradient method.

Specifically, given an image x as the input of the network, the output feature representation of x, denoted by $f(x; \theta)$, is obtained by capturing the activation in the last layer. Here θ are the network parameters, and we will use y to denote the ground truth value for the image which for image quality assessment is its quality score. Consequently, in our Siamese networks the output of the final layer is always a single scalar which we want to be indicative of the image quality. Since our aim is to rank the images, we apply the pairwise ranking hinge loss:

$$L(x_1, x_2; \theta) = \max\left(0, f(x_2; \theta) - f(x_1; \theta) + \varepsilon\right) \quad (1)$$

where ε is the margin. Here we assume without loss of generality that the rank of x_1 is higher than x_2. The gradient of the loss in Eq. 1 is given by:

$$\nabla_\theta L = \begin{cases} 0 & \text{if } f(x_2;\theta) - f(x_1;\theta) + \varepsilon \leq 0 \\ \nabla_\theta f(x_2;\theta) - \nabla_\theta f(x_1;\theta) & \text{otherwise.} \end{cases} \quad (2)$$

In other words, when the outcome of the network is in accordance with the ranking, the gradient is zero. When the outcome of the network is not in accordance we decrease the gradient of the higher and add the gradient of the lower score. Given this gradient of L with respect to model parameters θ, we can train the Siamese network using Stochastic Gradient Descent (SGD).

3.3. Efficient Siamese backpropagation

One drawback of Siamese networks is the redundant computation. Consider all possible image pairs constructed from three images. In a standard implementation all three images are passed twice through the network, because they each appear in two pairs. Since both branches of the Siamese network are identical, we are essentially doing twice the work necessary since any image need only be passed *once* through the network. It is exactly this idea that we exploit to render backpropagation more efficient. In fact, nothing prevents us from considering all possible pairs in the mini-batch, without hardly any additional computation. We add a new layer to the network that generates all possible pairs in a mini-batch at the end of the network right before computing the loss. This eliminates the problem of pair selection and boosts efficiency.

To approximate the speed-up of efficient Siamese backpropagation consider the following. If we have one reference image distorted by n levels of distortions in our training set, then for a traditional implementation of the Siamese network we would have to pass a total of $n^2 - n$ images through the network – which is twice the number of pairs you can generate with n images. Instead we propose to pass all images only a single time and consider all possible pairs only in the loss computation layer. This reduces computation to just n passes through the network. Therefore, the speed-up is equal to: $\frac{n^2-n}{n} = n - 1$. In the best scenario $n = M$, where M is equal to the number of images in the mini-batch, and hence the speed-up of this method would be in the order of the mini-batch size. Due to the high correlation among the set of all pairs in a mini-batch, we expect the final speedup in convergence to be lower.

To simplify notation in the following, we let $\hat{y}_i = f(x_i;\theta)$, where $f(x_i;\theta)$ is the output of a single branch of the Siamese network on input x_i. Now, for one pair of inputs the loss is:

$$L(x_1, x_2, l_{12}; \theta) = g(\hat{y}_1, \hat{y}_2, l_{12}), \quad (3)$$

where l_{12} is a label indicating the relationship between image 1 and 2 (for example, for ranking it indicates whether x_1 is of higher rank than x_2), and $\theta = \{\theta_1, \theta_2, \dots, \theta_k\}$ are all model parameters in the Siamese network. We omit the θ dependency in g for simplicity. The gradient of this loss function with respect to the model parameter θ is:

$$\nabla_\theta L = \frac{\partial g(\hat{y}_1, \hat{y}_2, l_{12})}{\partial \hat{y}_1} \nabla_\theta \hat{y}_1 + \frac{\partial g(\hat{y}_1, \hat{y}_2, l_{12})}{\partial \hat{y}_2} \nabla_\theta \hat{y}_2. \quad (4)$$

This gradient of L above is a sum since the model parameters are shared between both branches of the Siamese network and $\hat{y}_1$ and $\hat{y}_2$ are computed using exactly the same parameters.

Considering all pairs in a mini-batch, the loss is:

$$L = \sum_{i=1}^{M} \sum_{j>i}^{M} g(\hat{y}_i, \hat{y}_j, l_{ij}) \quad (5)$$

The gradient of the mini-batch loss with respect to parameter θ can then be written as:

$$\nabla_\theta L = \sum_{i=1}^{M} \sum_{j>i}^{M} \frac{\partial g(\hat{y}_i, \hat{y}_j, l_{ij})}{\partial \hat{y}_i} \nabla_\theta \hat{y}_i + \frac{\partial g(\hat{y}_i, \hat{y}_j, l_{ij})}{\partial \hat{y}_j} \nabla_\theta \hat{y}_j \quad (6)$$

We can now express the gradient of the loss function of the mini-batch in matrix form as:

$$\nabla_\theta L = \begin{bmatrix} \nabla_\theta \hat{y}_1 & \nabla_\theta \hat{y}_2 & \dots & \nabla_\theta \hat{y}_M \end{bmatrix} P \mathbf{1}_M \quad (7)$$

where $\mathbf{1}_M$ is the vector of all ones of length M. For a standard single-branch network, we would average the gradients for all batch samples to obtain the gradient of the mini-batch. This is equivalent to setting P to the identity matrix in Eq. 7 above. For Siamese networks where we consider all pairs in the mini-batch we obtain Eq. 6 by setting P to:

$$P = \begin{bmatrix} 0 & \frac{\partial g(\hat{y}_1, \hat{y}_2, l_{12})}{\partial \hat{y}_1} & \cdots & \frac{\partial g(\hat{y}_1, \hat{y}_M, l_{1M})}{\partial \hat{y}_1} \\ \frac{\partial g(\hat{y}_1, \hat{y}_2, l_{12})}{\partial \hat{y}_2} & 0 & \cdots & \frac{\partial g(\hat{y}_2, \hat{y}_M, l_{2M})}{\partial \hat{y}_2} \\ \vdots & \vdots & \ddots & \vdots \\ \frac{\partial g(\hat{y}_1, \hat{y}_M, l_{1M})}{\partial \hat{y}_M} & \cdots & \cdots & 0 \end{bmatrix} \quad (8)$$

The derivation until here is valid for any Siamese loss function of the form Eq. 3. For the specific case of the ranking hinge loss replace g in Eq. 8 with Eq. 1 and obtain:

$$P = \begin{bmatrix} 0 & a_{12} & \cdots & a_{1M} \\ a_{21} & 0 & \cdots & a_{2M} \\ \vdots & \vdots & \ddots & \vdots \\ a_{M1} & \cdots & a_{M(M-1)} & 0 \end{bmatrix}, \quad (9)$$

where

$$a_{ij} = \begin{cases} 0 & \text{if } l_{ij}(\hat{y}_j - \hat{y}_i) + \varepsilon \leq 0 \\ l_{ij} & \text{otherwise} \end{cases} \quad (10)$$

and $l_{ij} \in \{-1, 0, 1\}$ where 1 (-1) indicates that $y_i > y_j$ ($y_i < y_j$), and 0 that $y_i = y_j$ or that they cannot be compared as is the case with images corrupted with different distortions.

The above case considered a single distortion. Suppose instead we have D types of distortions in the training set. We can then compute the gradient of the loss using a block diagonal matrix as:

$$\nabla_\theta L = \begin{bmatrix} \nabla_\theta \hat{Y}^1 \ldots \nabla_\theta \hat{Y}^D \end{bmatrix} \begin{bmatrix} A^1 & 0 & \cdots & 0 \\ 0 & A^2 & \cdots & 0 \\ \vdots & \vdots & \ddots & \vdots \\ 0 & 0 & \cdots & A^d \end{bmatrix} \mathbf{1}_M \tag{11}$$

where

$$A^d = \begin{bmatrix} 0 & a_{12}^d & \cdots & a_{1M^d}^d \\ a_{21}^d & 0 & \cdots & a_{2M^d}^d \\ \vdots & \vdots & \ddots & \vdots \\ a_{M^d 1}^d & \cdots & a_{M^d(M^d-1)}^d & 0 \end{bmatrix}, \text{ and}$$

$$\nabla_\theta \hat{Y}^d = \begin{bmatrix} \nabla_\theta \hat{y}_{d1} & \cdots & \nabla_\theta \hat{y}_{dM} \end{bmatrix}. \tag{12}$$

where $\hat{y}_{mn}$ refers to the network output of the nth image with the mth distortion, $d \in \{1, 2, \ldots, D\}$, and $M = \sum M^d$ where M^d is the number of images with distortion d in the mini-batch. In the definition of A^d above, the a_{ij}^d are the gradient coefficients as in Eq. 10.

3.4. Fine-tuning for NR-IQA

After training a Siamese network to rank distorted images, we then extract a single branch from the network for fine-tuning. Given M images in mini-batch with human IQA measurements, we denote the ground truth quality score of the i-th image as y_i, and the predicted score from the network is $\hat{y}_i$, as above. We fine-tune the network using squared Euclidean distance as the loss function in place of the ranking loss used for the Siamese network:

$$L(y_i, \hat{y}_i) = \frac{1}{M} \sum_{i=1}^{M} (y_i - \hat{y}_i)^2 \tag{13}$$

4. Experimental results

In this section we report on a number of experiments designed to evaluate the performance of our approach with respect to baselines and the state-of-the-art in IQA. The code is available at https://github.com/xialeiliu/RankIQA.

4.1. Datasets

We use two types of datasets in our experiments: generic, non-IQA datasets for generating ranked images to train the Siamese network, and IQA datasets for fine-tuning and evaluation.
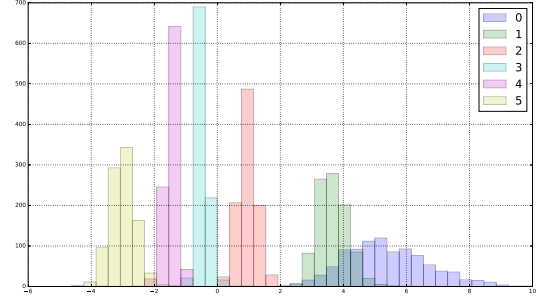

Figure 2. Siamese network output for JPEG distortion considering 6 levels. This graphs illustrate the fact that the Siamese network successfully manages to separate the different distortion levels.

IQA datasets. We perform experiments on two standard IQA benchmark datasets. The **LIVE** [28] consists of 808 images generated from 29 original images by distorting them with five types of distortion: Gaussian blur (GB), Gaussian noise (GN), JPEG compression (JPEG), JPEG2000 compression (JP2K) and fast fading (FF). The ground-truth Mean Opinion Score for each image is in the range [0, 100] and is estimated using annotations by 161 human annotators. The **TID2013** [22] dataset consists of 25 reference images with 3000 distorted images from 24 different distortion types at 5 degradation levels. Mean Opinion Scores are in the range [0, 9]. Distortion types include a range of noise, compression, and transmission artifacts. See the original publication for the list of specific distortion types.

Datasets for generating ranked pairs. To test on the LIVE database, we generate four types of distortions which are widely used and common : GB, GN, JPEG, and JP2K. To test on TID2013, we generate 17 out of a total of 24 distortions (apart from #3, #4, #12, #13, #20, #21, #24). For the distortions which we could not generate, we apply fine-tuning from the network trained from the other distortions. This was found to yield satisfactory results. We use two datasets for generating ranked image pairs.

The **Waterloo** dataset consists of 4,744 high quality natural images carefully chosen from the Internet. Additionally, we use the validation set of the **Places2** [45] dataset of 356 scene categories. There are 100 images per category in the validation set, for a total 36500 images. After distortion, we have many more distorted images for learning an image quality ranking embedding. The aim of using this dataset is to demonstrate that high-quality ranking embeddings can be learned using datasets not specifically designed for the IQA problem.

4.2. Experimental protocols

We investigate a number of network architectures and use standard IQA metrics to evaluate performance.

Network architectures. We evaluate three typical net-

work architectures varying from shallow to deep. We refer to them as: Shallow, AlexNet [14], and VGG-16 [30]. The shallow network has four convolutional layers and one fully connected layer. For AlexNet and VGG-16 we only change the number of outputs since our objective is to assign one score for each distorted image.

Strategy for training and testing. We randomly sample sub-images from the original high resolution images. We do this instead of scaling to avoid introducing distortions caused by interpolation or filtering. The size of sampled images is determined by each network. However, the large size of the input images is important since input sub-images should be at least 1/3 of the original images in order to capture context information. This is a serious limitation of the patch sampling approach that samples very small 32×32 patches from the original images. In our experiments, we sample 227×227 and 224×224 pixel images, depending on the network. We use the Caffe [10] framework and train using mini-batch Stochastic Gradient Descent (SGD) with an initial learning rate of 1e-4 for efficient Siamese network training and 1e-6 for fine-tuning. Training rates are decreased by a factor of 0.1 every 10K iterations for a total of 50K iterations. For both training phases we use ℓ_2 weight decay (weight 5e-4). During training we sample a single subimage from each training image per epoch.

When testing, we randomly sample 30 sub-images from the original images as suggested in [1]. The average of the outputs of the sub-regions is the final score for each image.

Evaluation protocols. Two evaluation metrics are traditionally used to evaluate the performance of IQA algorithms: the Linear Correlation Coefficient (LCC) and the Spearman Rank Order Correlation Coefficient (SROCC). LCC is a measure of the linear correlation between the ground truth and the predicted quality scores. Given N distorted images, the ground truth of i-th image is denoted by y_i, and the predicted score from the network is $\hat{y}_i$. The LCC is computed as:

$$LCC = \frac{\sum_{i=1}^{N}(y_i - \overline{y})(\hat{y}_i - \overline{\hat{y}})}{\sqrt{\sum_i^N (y_i - \overline{y})^2}\sqrt{\sum_i^N (\hat{y}_i - \overline{\hat{y}})^2}} \qquad (14)$$

where $\overline{y}$ and $\overline{\hat{y}}$ are the means of the ground truth and predicted quality scores, respectively.

Given N distorted images, the SROCC is computed as:

$$SROCC = 1 - \frac{6\sum_{i=1}^{N}(v_i - p_i)^2}{N(N^2 - 1)}, \qquad (15)$$

where v_i is the *rank* of the ground-truth IQA score y_i in the ground-truth scores, and p_i is the *rank* of $\hat{y}_i$ in the output scores for all N images. The SROCC measures the monotonic relationship between ground-truth and estimated IQA.
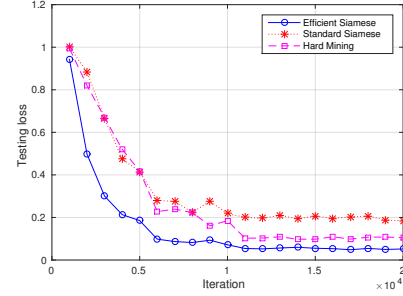

Figure 3. Convergence of ranking loss on JPEG distortion for our approach versus standard Siamese and hard-negative mining.

	Shallow	AlexNet	VGG-16
LCC	0.930	0.945	0.973
SROCC	0.937	0.949	0.974

Table 1. SROCC and LCC for our approach on LIVE using different networks.

4.3. Learning NR-IQA from rankings

We performed a number of experiments to evaluate the ability of Siamese networks to learn to capture image distortions from a large dataset of image quality rankings. In addition, we measure the impact of the efficient Siamese backpropagation approach described in section 3.3.

Siamese networks and IQA discrimination. To demonstrate the ability of our ranking networks to discriminate image quality, we trained our Siamese network on the Places2 validation set (without applying fine-tuning on IQA data) corrupted with five levels of a single distortion. We then used that network to predict image quality for synthetically-distorted images from the Waterloo dataset corrupted using the same five levels of the same distortion. The network outputs are plotted as histograms in Fig. 2 for the JPEG distortion[1]. In the plot, we divide the observations according to the true distortion level (indicated by the color of the histogram). The model discriminates different levels of distortions on Waterloo, even though the acquisition process and the scenes of the two datasets are totally different.

Efficient Siamese backpropagation. The objective of this experiment is to evaluate the efficiency of our Siamese backpropagation method. We compare our method to both standard random pair sampling, and a hard-negative mining method similar to [29].[2] For standard random pair sampling we randomly choose 36 pairs for each mini-batch from the training sets. For the hard negative mining strategy we start from 36 pairs in a mini-batch, and gradually increase the number of hard pairs every 5000 iterations. For our method we pass 72 images in each mini-batch. With these settings

---

[1]Graphs for the other distortions are in the supplementary material.
[2]We experimented with several hard-negative mining methods and found this to work best.

Method	#01	#02	#03	#04	#05	#06	#07	#08	#09	#10	#11	#12	#13
BLIINDS-II [23]	0.714	0.728	0.825	0.358	0.852	0.664	0.780	0.852	0.754	0.808	0.862	0.251	0.755
BRISQUE [19]	0.630	0.424	0.727	0.321	0.775	0.669	0.592	0.845	0.553	0.742	0.799	0.301	0.672
CORNIA-10K [40]	0.341	-0.196	0.689	0.184	0.607	-0.014	0.673	**0.896**	0.787	0.875	0.911	0.310	0.625
HOSA [36]	0.853	0.625	0.782	0.368	**0.905**	0.775	0.810	0.892	0.870	0.893	**0.932**	**0.747**	0.701
Baseline	0.605	0.468	0.761	0.232	0.704	0.590	0.559	0.782	0.639	0.772	0.817	0.571	0.725
RankIQA	**0.891**	**0.799**	**0.911**	**0.644**	0.873	**0.869**	**0.910**	0.835	**0.894**	**0.902**	0.923	0.579	0.431
RankIQA+FT	0.667	0.620	0.821	0.365	0.760	0.736	0.783	0.809	0.767	0.866	0.878	0.704	**0.810**
Method	#14	#15	#16	#17	#18	#19	#20	#21	#22	#23	#24	ALL	
BLIINDS-II [23]	0.081	0.371	0.159	-0.082	0.109	0.699	0.222	0.451	0.815	0.568	0.856	0.550	
BRISQUE [19]	0.175	0.184	0.155	0.125	0.032	0.560	0.282	0.680	0.804	0.715	0.800	0.562	
CORNIA-10K [40]	0.161	0.096	0.008	0.423	-0.055	0.259	0.606	0.555	0.592	0.759	0.903	0.651	
HOSA [36]	0.199	0.327	0.233	0.294	0.119	0.782	0.532	0.835	**0.855**	**0.801**	**0.905**	0.728	
Baseline	0.187	0.308	0.062	0.546	0.383	0.500	0.420	0.700	0.611	0.573	0.742	0.612	
RankIQA	0.463	**0.693**	**0.321**	**0.657**	0.622	**0.845**	0.609	**0.891**	0.788	0.727	0.768	0.623	
RankIQA+FT	**0.512**	0.622	0.268	0.613	**0.662**	0.619	**0.644**	0.800	0.779	0.629	0.859	**0.780**	

Table 2. Performance evaluation (SROCC) on the entire TID2013 database. The baseline approach is VGG16 fine-tuned directly on TID2013 data without using the Siamese net, RankIQA is VGG16 only fine-tuned for ranking using Siamese net on generated ranking data, and RankIQA+FT is our learning-from-ranking approach further fine-tuned on TID2013 data.

the computational costs of all three methods is equal, since at each iteration 72 images are passed through the network. We use AlexNet for this experiment. The comparison of convergence rates on JPEG[3] is shown in Fig. 3. The efficient Siamese backpropagation not only converges much faster, but also converges to a considerably lower loss.

Network performance analysis. Here we evaluate whether we can learn a useful image representation from large image ranking datasets. We randomly split on the original, high-quality images before distortion from the LIVE dataset into 80% training and 20% testing samples and compute the average LCC and SROCC scores on the testing set after training to convergence. This process is repeated ten times and the results are averaged. In Table 1 we compare results for three different networks: Shallow, AlexNet and VGG-16. We obtain the best results with the VGG-16 network, which is also the deepest network. This indicates learning from ranking makes it possible to train very deep networks efficiently without overfitting. These results are obtained by training from scratch, however we found that initializing the weights with a network pre-trained on ImageNet further improved the results. In the remainder of the experiments we thus use the VGG-16 network initialized with a pre-trained weights to train the ranking network in the following experiments.

Baseline performance analysis. In this experiment, we evaluate the effectiveness of using rankings to estimate image quality. We compare tree methods: fine-tuning the VGG-16 network initialized from ImageNet to obtain the mapping from images to their predicted scores (called Baseline), our method to train VGG-16 (initialized from ImageNet) on ranking database using all ranking dataset we generate (called RankIQA), and finally our RankIQA approach fine-tuned on the TID2013 database after training using ranked pairs of images (called RankIQA+FT).

We follow the experimental protocol used in HOSA [36]. The entire TID2013 database including all types of distortions is divided into 80% training images and 20% testing images according to the reference images. Thus, the same image can never appear in both training and test sets. The results are shown in Table 2, where ALL means testing all distortions together. All the experiments are performed 10 times and the average SROCC is reported[4]. From Table 2, we can draw several conclusions. First, it is hard to obtain good results by training a deep network directly on IQA data. This is seen in the Baseline results and is due to the scarcity of training data. Second, our RankIQA method achieves superior results on almost all individual distortions even without ever using the TID2013 dataset – which strongly demonstrates the effectiveness of training on ranking data. Slightly better results are obtained on ALL without comparing among different distortions during training the ranking network. The RankIQA-trained network alone does not provide accurate IQA scores (since it has never seen any) but does provide high correlation with the IQA scores as measured by SROCC. After fine-tuning on the TID2013 database (RankIQA+FT), we considerably improve the ALL score, and improve the baseline by 16%. However, in the fine-tuning process to optimize the ALL score the network balances the various distortions, and results decrease for several distortions.

4.4. Comparison with the state-of-the-art

We compare the performance of our method using the VGG-16 network with state-of-the-art methods. We perform experiments on the TID2013 and LIVE dataset.[5]

---

[3]Results for the other distortions are in the supplementary material.

[4]LCC results are provided in supplementary material.

[5]Results on CSIQ [15] and MLIVE [9] are in supplementary material.

	LCC	JP2K	JPEG	GN	GB	FF	ALL
FR-IQA	PSNR	0.873	0.876	0.926	0.779	0.87	0.856
	SSIM [35]	0.921	0.955	0.982	0.893	0.939	0.906
	FSIM [42]	0.91	0.985	0.976	0.978	0.912	0.96
	DCNN [17]	–	–	–	–	–	0.977
NR-IQA	DIVINE [21]	0.922	0.921	0.988	0.923	0.888	0.917
	BLIINDS-II [23]	0.935	0.968	0.98	0.938	0.896	0.93
	BRISQUE [19]	0.923	0.973	0.985	0.951	0.903	0.942
	CORNIA [40]	0.951	0.965	0.987	0.968	0.917	0.935
	CNN [11]	0.953	0.981	0.984	0.953	0.933	0.953
	SOM [43]	0.952	0.961	0.991	0.974	0.954	0.962
	DNN [2]	–	–	–	–	–	0.972
	RankIQA+FT	**0.975**	**0.986**	**0.994**	**0.988**	**0.960**	**0.982**

	SROCC	JP2K	JPEG	GN	BLUR	FF	ALL
FR-IQA	PSNR	0.87	0.885	0.942	0.763	0.874	0.866
	SSIM [35]	0.939	0.946	0.964	0.907	0.941	0.913
	FSIM [17]	0.97	0.981	0.967	0.972	0.949	0.964
	DCNN [17]	–	–	–	–	–	0.975
NR-IQA	DIVINE [21]	0.913	0.91	0.984	0.921	0.863	0.916
	BLIINDS-II [23]	0.929	0.942	0.969	0.923	0.889	0.931
	BRISQUE [19]	0.914	0.965	0.979	0.951	0.887	0.94
	CORNIA [40]	0.943	0.955	0.976	0.969	0.906	0.942
	CNN [11]	0.952	0.977	0.978	0.962	0.908	0.956
	SOM [43]	0.947	0.952	0.984	0.976	0.937	0.964
	DNN [2]	–	–	–	–	–	0.960
	RankIQA+FT	**0.970**	**0.978**	**0.991**	**0.988**	**0.954**	**0.981**

Table 3. LCC (above) and SROCC (below) evaluation on the LIVE dataset. We divide approaches into Full-reference (FR-IQA) and No-reference (IQA) techniques.

LCC	JP2K	JPEG	GN	GB	ALL
RankIQA+FT (Waterloo)	0.975	0.986	0.994	0.988	0.982
RankIQA+FT (Places2)	0.983	0.983	0.993	0.990	0.981
SROCC	**JP2K**	**JPEG**	**GN**	**GB**	**ALL**
RankIQA+FT (Waterloo)	0.970	0.978	0.991	0.988	0.981
RankIQA+FT (Places2)	0.970	0.982	0.990	0.988	0.980

Table 4. SROCC and LCC results of models trained on the Waterloo and Places2 datasets, testing on LIVE.

Evaluation on TID2013. Table 2 also includes results of state-of-the-art methods. We see that for several very challenging distortions (14 to 18), where all other methods fail, we obtain satisfactory results. For individual distortions, there is a huge gap between our RankIQA method and other IQA methods on most distortions. The state-of-the-art method HOSA performs slightly better than our methods on 6 out of 24 distortions. For all distortions, our method RankIQA+FT achieves about 5% higher than HOSA. Our methods perform well on distortions which are not included when training the ranking network, which indicates that different distortions share some common representation and training the network jointly on all distortions.

Evaluation on LIVE. As done in [11, 43], we randomly split the reference images on LIVE dataset into 80% training samples and 20% testing, and compute the average LCC and SROCC scores on the testing set after training to convergence. This process is repeated ten times and the results are averaged. These results are shown in Table 3. The best method for each dataset is indicated in bold. The column indicated with ALL means we combine all five distortions together on LIVE dataset to train and test the model. For fair comparison with the state-of-the-art, we train our ranking model on four distortions except FF, but we fine-tune our model on all five distortions in the LIVE dataset to compute ALL. Our approach achieves about 1% better than the best results reported on ALL distortions for LCC. Similar conclusions are obtained for SROCC. This indicates that

our method outperforms existing work including the current state-of-the-art NR-IQA method SOM [43] and DNN [2], and also state-of-the-art FR-IQA method DCNN [17]. *To the best of our knowledge this is the first time that an NR-IQA method surpasses the performance of FR-IQA methods (which have access to the undistorted reference image) on all LIVE distortions using the LCC and SROCC evaluation method.*

4.5. Independence from IQA training data

This final experiment is to demonstrate that our framework can be also trained on non-IQA datasets. In the previous experiment the network is trained from high-quality images of the Waterloo dataset. Instead here we use the validation set of the Places2 dataset to generate ranked images in place of the Waterloo dataset. The Places2 dataset is of lower quality than Waterloo and is not designed for IQA research. As in the previous experiment, the final image quality scores are predicted by fine-tuning on the LIVE dataset. The performance of this model is compared with the results trained on Waterloo in Table 4. The SROCC and LCC values are very similar, demonstrating that our approach can be learnt from arbitrary, non-IQA data.

5. Conclusions

To address the scarcity of IQA data we have proposed a method which learns from ranked image datasets. Since this data can be generated in abundance we can train deeper and wider networks than previous work. In addition, we have proposed a method for efficient backpropagation in Siamese networks which circumvents the need for hard-negative mining. Comparison with standard pair sampling and hard-negative sampling shows that our method converges faster and to a lower loss. Results on LIVE and TID2013 datasets show that our NR-IQA approach obtains superior results compared to existing NR-IQA techniques and even FR-IQA methods.

References

[1] S. Bianco, L. Celona, P. Napoletano, and R. Schettini. On the use of deep learning for blind image quality assessment. *arXiv preprint arXiv:1602.05531*, 2016. 2, 6

[2] S. Bosse, D. Maniry, T. Wiegand, and W. Samek. A deep neural network for image quality assessment. In *Image Processing (ICIP), 2016 IEEE International Conference on*, pages 3773–3777. IEEE, 2016. 2, 8

[3] W. Chen, T.-Y. Liu, Y. Lan, Z.-M. Ma, and H. Li. Ranking measures and loss functions in learning to rank. In *Advances in Neural Information Processing Systems*, pages 315–323, 2009. 2

[4] A. Chetouani, A. Beghdadi, S. Chen, and G. Mostafaoui. A novel free reference image quality metric using neural network approach. In *Proc. Int. Workshop Video Process. Qual. Metrics Cons. Electrn*, pages 1–4, 2010. 2

[5] S. Chopra, R. Hadsell, and Y. LeCun. Learning a similarity metric discriminatively, with application to face verification. In *Computer Vision and Pattern Recognition, 2005. CVPR 2005. IEEE Computer Society Conference on*, volume 1, pages 539–546. IEEE, 2005. 2, 3

[6] F. Gao, D. Tao, X. Gao, and X. Li. Learning to rank for blind image quality assessment. *Neural Networks and Learning Systems, IEEE Transactions on*, 26(10):2275–2290, 2015. 2

[7] S. A. Golestaneh and D. M. Chandler. No-reference quality assessment of jpeg images via a quality relevance map. *Signal Processing Letters, IEEE*, 21(2):155–158, 2014. 1

[8] K. He, X. Zhang, S. Ren, and J. Sun. Deep residual learning for image recognition. In *Proceedings of the IEEE Conference on Computer Vision and Pattern Recognition*, 2016. 1

[9] D. Jayaraman, A. Mittal, A. K. Moorthy, and A. C. Bovik. Objective quality assessment of multiply distorted images. In *Signals, Systems and Computers (ASILOMAR), 2012 Conference Record of the Forty Sixth Asilomar Conference on*, pages 1693–1697. IEEE, 2012. 7

[10] Y. Jia, E. Shelhamer, J. Donahue, S. Karayev, J. Long, R. Girshick, S. Guadarrama, and T. Darrell. Caffe: Convolutional architecture for fast feature embedding. *arXiv preprint arXiv:1408.5093*, 2014. 6

[11] L. Kang, P. Ye, Y. Li, and D. Doermann. Convolutional neural networks for no-reference image quality assessment. In *Proceedings of the IEEE Conference on Computer Vision and Pattern Recognition*, pages 1733–1740, 2014. 2, 8

[12] L. Kang, P. Ye, Y. Li, and D. Doermann. Simultaneous estimation of image quality and distortion via multi-task convolutional neural networks. In *Image Processing (ICIP), 2015 IEEE International Conference on*, pages 2791–2795. IEEE, 2015. 2, 3

[13] A. K. Katsaggelos. *Digital image restoration*. Springer Publishing Company, Incorporated, 2012. 1

[14] A. Krizhevsky, I. Sutskever, and G. E. Hinton. Imagenet classification with deep convolutional neural networks. In *Advances in neural information processing systems*, pages 1097–1105, 2012. 1, 6

[15] E. C. Larson and D. M. Chandler. Most apparent distortion: full-reference image quality assessment and the role of strat-egy. *Journal of Electronic Imaging*, 19(1):011006–011006, 2010. 7

[16] Y. LeCun, L. Bottou, Y. Bengio, and P. Haffner. Gradient-based learning applied to document recognition. *Proceedings of the IEEE*, 86(11):2278–2324, 1998. 1

[17] Y. Liang, J. Wang, X. Wan, Y. Gong, and N. Zheng. Image quality assessment using similar scene as reference. In *European Conference on Computer Vision*, pages 3–18. Springer, 2016. 2, 8

[18] L. Liu, H. Dong, H. Huang, and A. C. Bovik. No-reference image quality assessment in curvelet domain. *Signal Processing: Image Communication*, 29(4):494–505, 2014. 1, 2

[19] A. Mittal, A. K. Moorthy, and A. C. Bovik. No-reference image quality assessment in the spatial domain. *Image Processing, IEEE Transactions on*, 21(12):4695–4708, 2012. 1, 2, 7, 8

[20] A. K. Moorthy and A. C. Bovik. A two-step framework for constructing blind image quality indices. *Signal Processing Letters, IEEE*, 17(5):513–516, 2010. 1, 2

[21] A. K. Moorthy and A. C. Bovik. Blind image quality assessment: From natural scene statistics to perceptual quality. *IEEE Transactions on Image Processing*, 20(12):3350–3364, 2011. 8

[22] N. Ponomarenko, O. Ieremeiev, V. Lukin, K. Egiazarian, L. Jin, J. Astola, B. Vozel, K. Chehdi, M. Carli, F. Battisti, et al. Color image database tid2013: Peculiarities and preliminary results. In *Visual Information Processing (EUVIP), 2013 4th European Workshop on*, pages 106–111. IEEE, 2013. 1, 5

[23] M. A. Saad, A. C. Bovik, and C. Charrier. Blind image quality assessment: A natural scene statistics approach in the dct domain. *Image Processing, IEEE Transactions on*, 21(8):3339–3352, 2012. 1, 2, 7, 8

[24] F. Schroff, D. Kalenichenko, and J. Philbin. Facenet: A unified embedding for face recognition and clustering. In *Proceedings of the IEEE Conference on Computer Vision and Pattern Recognition*, pages 815–823, 2015. 3

[25] D. Sculley. Large scale learning to rank. In *NIPS Workshop on Advances in Ranking*, pages 1–6, 2009. 2

[26] K. Sharifi and A. Leon-Garcia. Estimation of shape parameter for generalized gaussian distributions in subband decompositions of video. *Circuits and Systems for Video Technology, IEEE Transactions on*, 5(1):52–56, 1995. 2

[27] H. R. Sheikh, M. F. Sabir, and A. C. Bovik. A statistical evaluation of recent full reference image quality assessment algorithms. *Image Processing, IEEE Transactions on*, 15(11):3440–3451, 2006. 1

[28] H. R. Sheikh, Z. Wang, L. Cormack, and A. C. Bovik. Live image quality assessment database. http://live.ece.utexas.edu/research/quality. 5

[29] E. Simo-Serra, E. Trulls, L. Ferraz, I. Kokkinos, P. Fua, and F. Moreno-Noguer. Discriminative learning of deep convolutional feature point descriptors. In *Proceedings of the IEEE International Conference on Computer Vision*, pages 118–126, 2015. 3, 6

[30] K. Simonyan and A. Zisserman. Very deep convolutional networks for large-scale image recognition. *ICLR*, 2015. 6

[31] H. O. Song, Y. Xiang, S. Jegelka, and S. Savarese. Deep metric learning via lifted structured feature embedding. In *Proceedings of the IEEE Conference on Computer Vision and Pattern Recognition*, 2016. 3

[32] J. Van Ouwerkerk. Image super-resolution survey. *Image and Vision Computing*, 24(10):1039–1052, 2006. 1

[33] X. Wang and A. Gupta. Unsupervised learning of visual representations using videos. In *Proceedings of the IEEE International Conference on Computer Vision*, pages 2794–2802, 2015. 3

[34] Z. Wang, A. C. Bovik, and L. Lu. Why is image quality assessment so difficult? In *Acoustics, Speech, and Signal Processing (ICASSP), 2002 IEEE International Conference on*, volume 4, pages IV–3313. IEEE, 2002. 1

[35] Z. Wang, A. C. Bovik, H. R. Sheikh, and E. P. Simoncelli. Image quality assessment: from error visibility to structural similarity. *IEEE transactions on image processing*, 13(4):600–612, 2004. 8

[36] J. Xu, P. Ye, Q. Li, H. Du, Y. Liu, and D. Doermann. Blind image quality assessment based on high order statistics aggregation. *IEEE Transactions on Image Processing*, 25(9):4444–4457, 2016. 7

[37] J. Yan, S. Lin, S. B. Kang, and X. Tang. A learning-to-rank approach for image color enhancement. In *Computer Vision and Pattern Recognition (CVPR), 2014 IEEE Conference on*, pages 2987–2994. IEEE, 2014. 1

[38] Q. Yan, Y. Xu, and X. Yang. No-reference image blur assessment based on gradient profile sharpness. In *Broadband Multimedia Systems and Broadcasting (BMSB), 2013 IEEE International Symposium on*, pages 1–4. IEEE, 2013. 1

[39] P. Ye and D. Doermann. No-reference image quality assessment using visual codebooks. *Image Processing, IEEE Transactions on*, 21(7):3129–3138, 2012. 2

[40] P. Ye, J. Kumar, L. Kang, and D. Doermann. Unsupervised feature learning framework for no-reference image quality assessment. In *Computer Vision and Pattern Recognition (CVPR), 2012 IEEE Conference on*, pages 1098–1105. IEEE, 2012. 2, 7, 8

[41] S. Zagoruyko and N. Komodakis. Learning to compare image patches via convolutional neural networks. In *Proceedings of the IEEE Conference on Computer Vision and Pattern Recognition*, pages 4353–4361, 2015. 2

[42] L. Zhang, L. Zhang, X. Mou, and D. Zhang. Fsim: a feature similarity index for image quality assessment. *IEEE transactions on Image Processing*, 20(8):2378–2386, 2011. 8

[43] P. Zhang, W. Zhou, L. Wu, and H. Li. Som: Semantic obviousness metric for image quality assessment. In *Proceedings of the IEEE Conference on Computer Vision and Pattern Recognition*, pages 2394–2402, 2015. 2, 8

[44] Q. Zhang, Z. Ji, S. Lilong, and I. Ovsiannikov. Label-free non-reference image quality assessment via deep neural network, Nov. 3 2015. US Patent App. 14/931,843. 2

[45] B. Zhou, A. Lapedriza, J. Xiao, A. Torralba, and A. Oliva. Learning deep features for scene recognition using places database. In *Advances in neural information processing systems*, pages 487–495, 2014. 5